g-Tensor of the Neutral Flavin Radical Cofactor of DNA Photolyase Revealed by 360-GHz Electron Paramagnetic Resonance Spectroscopy

Martin R. Fuchs,[†] Erik Schleicher,[‡] Alexander Schnegg,[†] Christopher W. M. Kay,[†] Jens T. Törring,[†] Robert Bittl,[†] Adelbert Bacher,[‡] Gerald Richter,[‡] Klaus Möbius,[†] and Stefan Weber*[,†]

Institute of Experimental Physics, Free University Berlin, 14195 Berlin, Germany, and Institute of Organic Chemistry and Biochemistry, Technical University Munich, 85747 Garching, Germany

Received: April 22, 2002

The flavin cofactor of *Escherichia coli* DNA photolyase in its neutral radical form, FADH•, was investigated by high-frequency/high-field continuous-wave electron paramagnetic resonance at 360 GHz. The data presented are the first flavin radical spectra where the full rhombic symmetry of the **g**-tensor is resolved. A fit of the spectrum yields accurate principal values of **g**, which show only a small anisotropy: $g_X = 2.004\ 31(5)$, $g_Y = 2.003\ 60(5)$ and $g_Z = 2.002\ 17(7)$. The hyperfine splitting observed in the g_Y region could be assigned to a hyperfine tensor component of the H(5) proton in the 7,8-dimethyl isoalloxazine moiety of FADH•. From a comparison of this effective hyperfine coupling with the principal value obtained from pulsed (Davies) electron−nuclear double resonance, the orientation of the **g**-tensor principal axes with respect to the H(5) hyperfine principal axes could be derived. Remaining ambiguities in the sign of the angle between the principal axes of **g** and the molecular axes are discussed by taking into account results from **g**-tensor calculations using density functional theory and semiempirical AM1 based methods.

Introduction

Flavins are distributed widely in nature as cofactors in enzymes that catalyze a broad variety of biochemical reactions.[1−4] These range from the biosynthesis and degradation of metabolic intermediates to one- and two-electron-transfer processes from and to redox centers. Flavins can exist in three different oxidation states: oxidized flavoquinone, one-electron reduced flavin semiquinone radical, and two-electron reduced flavo-1,5-dihydroquinone form. In all three redox states, flavins are amphoteric molecules,[2] i.e., depending on the pH conditions they can exist as anions, neutral molecules or cations.

The involvement of paramagnetic flavin semiquinone intermediates in flavoenzyme-catalyzed reactions has been studied extensively (for a review, see ref 5). In photolyases, for example, a neutral flavin adenine dinucleotide radical, FADH•, is created in the course of cofactor photoreduction and in photorepair of UV-damaged DNA.[6−12] A detailed knowledge of the electronic structure of FADH• and its interactions with the protein environment is therefore indispensable for a thorough understanding of these important photoprocesses.

In the studies of the paramagnetic flavin species, application of electron paramagnetic resonance (EPR) has traditionally yielded valuable information on the structures and the properties of these radicals.[13] It has been particularly useful to distinguish the anionic and neutral forms. Electron−nuclear double resonance (ENDOR) with its increased spectral resolution has provided information on the molecular structure and electronic distribution on model flavin and flavoprotein radicals.[14−22] Together with pulsed EPR techniques,[23−25] these methods enable—via the detection of hyperfine coupling constants—to map the spin density distribution on the tricyclic heteronuclear aromatic flavin ring system. Such information is prerequisite for the determination of sites that may participate in electron-transfer reactions of flavoenzymes.

Little information, however, is available on the **g**-tensor of flavins, so far,[19,21,26,27] because high microwave frequencies and correspondingly strong magnetic fields are required to resolve **g**-anisotropies that are relatively small and therefore difficult to detect at conventional EPR frequencies below 100 GHz due to the large inhomogeneous line width of flavin semiquinones. Following the first EPR experiments at 150 GHz,[28] high-frequency/high-field EPR spectrometers operating at frequencies in the range of 100 to 250 GHz have been constructed.[29−32] However, only very few spectrometers have been described so far that operate at even higher frequencies up to 600 GHz.[33−40] Their construction requires drastically increased experimental difficulties to be overcome, often approaching the limits of current microwave and cryomagnet technologies. This effort is, however, well rewarded considering the fact that the **g**-tensor provides important information about paramagnetic species. It represents a global probe of the spatial and electronic structure of the paramagnetic centers and allows for an identification of a specific radical. Moreover, knowledge of the **g**-tensor principal values and principal axes of flavins is needed for obtaining structural information of transient radical pairs that are created in the course of electron-transfer reactions in flavoenzyme-mediated biochemical processes.

With the recent availability of powerful high-field/high-frequency EPR instrumentation—up to 14 T/360 GHz in our laboratory[40] —it is now possible to perform experiments to resolve the small **g**-anisotropy of flavin semiquinones. In the

* To whom correspondence should be addressed. Institute of Experimental Physics, Free University Berlin, Arnimallee 14, 14195 Berlin, Germany. Tel.: 49-30-838-56139; Fax: 49-30-838-56046. E-mail: Stefan.Weber@physik.fu-berlin.de.

[†] Institute of Experimental Physics, Free University Berlin.

[‡] Institute of Organic Chemistry and Biochemistry, Technical University Munich.

10.1021/jp0259869 CCC: $22.00
Published on Web 08/02/2002

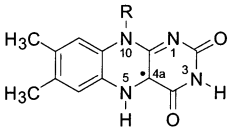

Figure 1. Molecular structure and IUPAC numbering scheme of the 7,8-dimethyl isoalloxazine moiety of flavin semiquinones.

present study we will focus on the redox-active flavin cofactor of *Escherichia coli* DNA photolyase that is reversibly transformed into its neutral radical form, FADH•, upon isolation and purification of the enzyme in an aerobic environment.[41−43] The FADH• radical thus produced can be viewed as a naturally occurring spin probe at the active site of the enzyme. Proton hyperfine couplings have been measured and assigned in a recent 9-GHz EPR/ENDOR study of the isolated protein.[21] A theoretical study on the electronic structure of the flavin cofactor in DNA photolyase has also been provided.[44] In a previous 94.5-GHz EPR experiment[21] the isotropic *g*-value of FADH• has been measured but the full **g**-anisotropy could not be resolved. Here, we apply 360-GHz EPR with its drastically increased spectral resolution to accurately determine the full rhombic symmetry of the **g**-tensor of FADH•. Additionally, for the first time, information on the orientation of the principal axes of **g** with respect to the molecular frame of the flavin's redox-active 7,8-dimethyl isoalloxazine moiety is obtained from a comparison of the observed single hyperfine splitting assigned to H(5) of FADH• (see Figure 1) with that measured by pulsed Davies ENDOR. The remaining ambiguity in the sign of the angle defining the rotation of the principal axes of **g** with respect to those of the H(5) hyperfine tensor is discussed taking into account first quantum-chemical calculations of the **g**-tensor of FADH• using semiempirical AM1 based and density functional theory (DFT) methods. Such data is crucial for a quantitative interpretation of the published radical-pair spectra in photolyases[45−50] and other flavoenzymes (see, e.g., refs 26,27).

Materials and Methods

Preparation and Isolation of DNA Photolyase. All experiments presented in this contribution were performed on the E109A mutant of DNA photolyase from *E. coli*. Replacement of the glutamic acid E109 by alanine results in an enzyme devoid of the light-harvesting cofactor, 5,10-methenyltetrahydrofolylpolyglutamate, which has the same EPR spectral properties as the wild-type protein.[21,22] Construction of the E109A mutant and its purification are described elsewhere (Schleicher et al., manuscript in preparation). The enzyme concentration of 1.5 mM was calculated on the basis of FADH• optical absorption at 580 nm ($\epsilon_{580} = 4800\ M^{-1}\ cm^{-1}$).[51] Absorption spectra were recorded at room temperature using a Shimadzu UV-1600PC (Shimadzu, Columbia, MD) spectrophotometer.

Samples were transferred into the desired buffer (50 mM HEPES in H_2O/glycerol (pH 7.0) or HEPES in D_2O/glycerol-D_3 (pD 7.0)) by dilution and ultrafiltration through C30 microconcentrators at 4 °C. This cycle was repeated five times to give a final buffer or D_2O enrichment of 95−99%.

EPR Instrumentation. The general setup of the 360-GHz EPR spectrometer has been described previously.[40] The microwave source consists of a phase-locked frequency-tripled 120.01-GHz Gunn diode oscillator yielding a microwave signal frequency of 360.03 GHz. The microwave heterodyne detector consists of a subharmonic mixer operating at the second harmonic frequency of a local oscillator input provided by a phase-locked frequency-doubled 90.31-GHz Gunn oscillator. The resulting intermediate frequency of 1.21 GHz was finally down-converted with a low-frequency reference oscillator. The transmission line is arranged in an induction-mode setup exploiting the linear polarization of the free-space Gaussian beam to isolate the detection arm from the excitation arm by approximately 30 dB.[36,40] By using exclusively reflective optics for microwave beam refocusing and by employing an oversized corrugated waveguide within the superconducting 14-T magnet warm bore, losses, cross-polarization, and standing waves could be reduced to a minimum. Microwave attenuation was achieved by insertion of PVC plates (5 mm thickness) tilted at a slight angle to prevent buildup of standing waves.

The resonator consists of a semi-confocal Fabry-Pérot-type cavity that is typically operated in a TEM_{006} mode. A free-standing copper mesh is used to couple microwaves into the resonant structure. Under dim light conditions, the protein fluid sample was soaked into a piece of cellulose tissue (2 × 2 mm, sample volume: approximately 1 μL) and placed on the curved mirror surface of the resonator, which was then immersed in a static helium contact cryostat (Oxford Instruments CF1200) and cooled to 200 K (frozen solution). The six-line EPR spectrum of a Mn(II)/MgO standard in a polystyrene matrix (to prevent mixing with the protein sample), placed near the sample in the cavity, was recorded simultaneously for *g*-factor calibration and subsequently subtracted from the EPR spectrum in order to obtain the undistorted spectrum of the sample. As the current setup does not contain a phase-shifter, the phase of the measured signals was tuned off-line numerically to a pure absorption signal by a Hilbert transformation.[52]

Simulation of EPR Spectra. The EPR powder spectra have been analyzed using a program for simulation and fitting of spectra with anisotropic **g**-tensor and hyperfine tensors, $\mathbf{A}_i$. The spectra were calculated by computing the resonant magnetic field position at the given microwave frequency by numerical diagonalization of the Hamiltonian containing the electron Zeeman and various hyperfine terms

$$H = H_{\mathrm{Zeeman}} + H_{\mathrm{hyperfine}} = \mu_{\mathrm{B}}\, \boldsymbol{B}\mathbf{g}\boldsymbol{S} + \sum_i \boldsymbol{S}\mathbf{A}_i\boldsymbol{I}_i \qquad (1)$$

which is dependent on the orientation of the tensors with respect to the external magnetic field vector $\boldsymbol{B}$. $\boldsymbol{S}$ and $\boldsymbol{I}_i$ are the electronic and the nuclear spin vector operators, respectively, and μ_{B} is the Bohr magneton. The superposition of all orientations for the randomly oriented powder-like sample was performed using an igloo approach[53] typically using 500 grid points. No restrictions for the relative orientations of the principal axes of the different tensors were imposed. The principal axes system of **g** served as a reference system. To calculate the spectral transitions, a numerical diagonalization (Matlab, The Mathworks, Inc.) was performed to obtain eigenvalues and eigenstates of *H*. The transition probability between corresponding energy levels was derived following the treatment described in the literature.[54,55]

Residual inherent line widths observed in powder spectra can contain contributions from unresolved hyperfine couplings and also **g**-strain effects, both of which can be orientation dependent. Therefore, to account for line broadening due to **g**-strain or unresolved hyperfine couplings with anisotropic tensors collinear to the **g**-tensor, the line widths were taken to lie on an ellipsoid whose principal axes are collinear with those of the **g**-tensor.

A nonlinear least-squares routine based on a trust-region reflective Newton algorithm (Matlab, The Mathworks, Inc.) was used to find the optimum parameter set for simulating a given experimental spectrum. The starting parameter set has been

systematically varied over a wide range of physically plausible values to avoid convergence of the optimization procedure in a local minimum. The error margins of the fitted parameters are the confidence intervals obtained from the fitting routine.

MO Calculations of the g-Tensor. Calculations of the principal values and axes of the neutral flavin radical **g**-tensor have been performed using semiempirical AM1 and DFT methods. As a model for FADH• in these computations, lumiflavin was geometry-optimized utilizing the Becke3 exchange functional combined with the Lee−Yang−Parr correlation functional, B3LYP,[56−58] as implemented in Gaussian 98.[59] The basis set used was 6-31G*.

For the semiempirical calculation of the **g**-tensor, the method described by Törring and co-workers[60] has been used. It employs the results of an AMPAC version 5.0 (Semichem, Shawnee, KS) semiempirical AM1[61] restricted Hartree−Fock computation using a perturbation theory approach similar to the one proposed by Stone,[62] but modified to include effects due to multi-center contributions, corrected energy denominators and relativistic corrections.

DFT calculations of the **g**-tensor were performed using the ADF package (ADF Release 2000.02, Scientific Computing and Modeling NV, Theoretical Chemistry, Vrije Universiteit Amsterdam, The Netherlands)[63−66] at the spin−orbit relativistic zero-order regular approximation (ZORA) level[67,68] using the popular BP86 functional[69,70] and the ADF basis set II (double-ξ).

For a qualitative discussion of **g**-tensor anisotropies of heteronuclear systems with large spin−orbit couplings, these rather extensive computations can be replaced by approximate expressions derived by Stone[62] (see eq 2 in Results and Discussion).

Results and Discussion

The 360.03-GHz EPR signal of the flavin cofactor in its stable neutral radical form, FADH•, in *E. coli* DNA photolyase recorded at $T = 200$ K is shown in Figure 2 (traces A and C). The frozen sample gives rise to a well-resolved line shape characteristic of a randomly oriented radical with a **g**-tensor of rhombic symmetry ($g_X \neq g_Y \neq g_Z$; X, Y, and Z designate the principal axes of the **g**-tensor). This is a major progress to previously published 94.5-GHz EPR results on the same sample[21] where the g_X- and g_Y-features remained unresolved owing to the inhomogeneous hyperfine line width still exceeding the Zeeman-anisotropy of FADH•. From a spectral simulation of the 360.03-GHz EPR signal, the three principal values of the FADH•'s **g**-tensor were determined, $g_X = 2.00431(5)$, $g_Y = 2.00360(5)$, and $g_Z = 2.00217(7)$. The resulting average value $g_{iso} = 2.00336(5)$ confirms that obtained from 94.5-GHz EPR[21] on the same sample. A larger value, $g_{iso} = 2.0042$, has been reported from 35-GHz EPR on the anionic flavin semiquinone in monoamine oxidase B.[19] Even larger values ($2.0045 \leq g_{iso} \leq 2.005$) have been obtained from multi-frequency EPR studies of the flavin mononucleotide (FMNH) cofactor, in its neutral radical state, interacting with the iron−sulfur complex in the enzyme trimethylamine dehydrogenase.[26,27] In this system, however, an accurate determination of the principal values of the **g**-tensor is hampered by additional line broadening due to magnetic interaction (exchange and dipolar coupling) of the FMNH• radical with the paramagnetic $[4Fe-4S]^{1+}$ cluster and by spectral overlap of their individual signal contributions. It is also possible that the proximity of the iron−sulfur complex significantly alters the FMNH cofactor surroundings compared to that of an isolated FMNH, resulting in the observed shift of

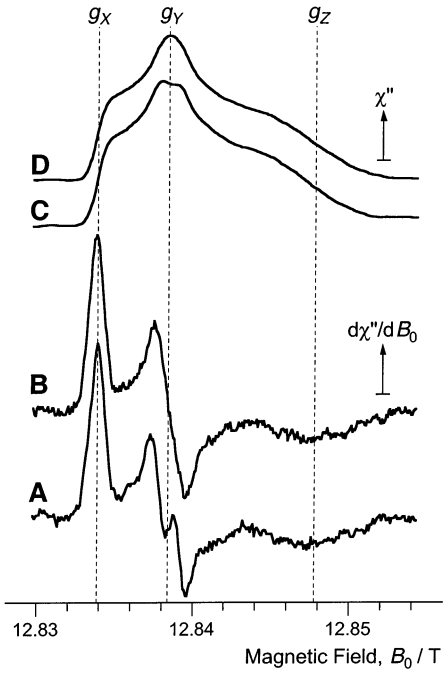

Figure 2. 360.03-GHz continuous-wave EPR frozen-solution spectra of the neutral flavin radical, FADH•, in DNA photolyase from *E. coli* in protonated (trace A) and deuterated (trace B) buffer. Spectra were recorded in the first-derivative mode (traces A and B) at 200 K with microwave power 1 μW, modulation amplitude 0.4 mT (1.8 kHz modulation frequency). The calibration of the magnetic field axis was performed for trace A according to the procedure outlined in the Materials and Methods section. Because the field standard lines in the spectrum of the deuterated sample, trace B, were too small to be detected, the same magnetic-field-to-magnet-coil-current ratio was used for scaling as determined for trace A, and trace B subsequently aligned to trace A at the g_X-position. The traces A and B have been integrated to yield traces C and D, respectively.

g_{iso}. Such possible complications do not apply here as the 360-GHz EPR spectrum of the isolated flavin cofactor in its DNA photolyase protein environment is recorded unperturbed by other paramagnetic centers.

For planar π-radicals in aromatic systems, the Z-axis of **g** is perpendicular to the molecular plane. According to established **g**-tensor theory,[62] this out-of-plane component should be equal to the free-electron value ($g_e = 2.002\,319$). This is almost observed for FADH•, $g_Z = 2.002\,17(7)$; the small deviation is due to relativistic effects. The in-plane components g_X and g_Y are shifted by $\Delta g_X = g_X - g_e$ and $\Delta g_Y = g_Y - g_e$ toward higher values. For π-radicals with heavy heteroatoms such as nitrogen or oxygen, these shifts originate predominantly from excitations of an electron from a nonbonding lone-pair orbital at the heteroatoms into the half-filled π*-orbital.[62] For the component along X, Δg_X can be approximated by

$$\Delta g_X = 2 \sum_i \xi_i \rho_i^{\pi} c_{iY}^2 / \Delta E_{in\pi^*} \qquad (2)$$

where ξ_i is the spin−orbit coupling constant of nucleus i of the π-system, ρ_i^{π} the π-spin density, and c_{iY} the orbital coefficient of the p_{iY} contribution to the lone pair orbital of the respective nucleus.[62] $\Delta E_{in\pi^*}$ is the excitation energy for raising the lone pair electron at nucleus i into the π*-orbital. An analogous expression is obtained for Δg_Y. The small deviations of g_X and g_Y from the free-electron value observed for FADH• (see Table 1) are due to the fact that spin density in the neutral flavin radical is mainly localized on C(4a) and, to a lesser extent, on N(5) and N(10).[44] Carbons and nitrogens have considerably lower

TABLE 1: EPR Parameters Used in the Simulation of 360.03-GHz EPR Spectra of the Neutral Flavin Radical Bound to DNA Photolyase

g-tensor[a]	$g_X = 2.00431(5)$
	$g_Y = 2.00360(5)$
	$g_Z = 2.00217(7)$
inhomogeneous (residual) line width[a]	$\Gamma_X = 0.73(4)$ mT
	$\Gamma_Y = 0.94(4)$ mT
	$\Gamma_Z = 1.2(1)$ mT
hyperfine coupling ^{14}N(5)[b]	$A_\perp = -0.06$ mT
	$A_\parallel = 1.53$ mT
hyperfine coupling ^{14}N(10)[b]	$A_\perp = 0.04$ mT
	$A_\parallel = 0.83$ mT
hyperfine coupling ^{1}H(5)[c]	$A_x = -0.30(1)$ mT
	$A_y = -1.33(1)$ mT
	$A_z = -0.89(1)$ mT

[a] The error margins given are the confidence intervals obtained from the fitting routine. In the case of g_X and g_Y, the error is due to uncertainties in the isotropic *g*-value of the Mn(II)/MgO field standard.[32] [b] Data taken from ref 44. [c] Data taken from (Weber et al., manuscript in preparation).

spin−orbit coupling constants than oxygen (ξ = 28, 76, and 151 cm^{-1} for C, N, and O, respectively; ref 71, p 138) resulting in a rather small **g**-anisotropy as compared to that of, e.g., tyrosine or quinone radicals where large π-spin density is found on the oxygen(s).

Further inspection of the 360.03-GHz EPR spectrum, Figure 2 (trace A), reveals a 1.30-mT splitting at the g_Y turning point of the powder pattern, which disappears upon replacement of the protonated for deuterated buffer, Figure 2 (trace B). Upon buffer deuteration, the exchangeable protons at N(3) and N(5) (for the IUPAC numbering scheme, see Figure 1) are replaced by deuterons. This results in a reduced overall EPR line width because of the 6.5-fold smaller nuclear moment of a deuteron as compared to that of a proton. From ENDOR studies of flavins[15] and DFT calculations of FADH• proton hyperfine couplings[44] it is known that the hyperfine coupling of H(3) is considerably smaller than that of H(5) and, therefore, cannot account for the large splitting observed in trace A of Figure 2. Hence, this feature is attributed to the hyperfine splitting of the more strongly coupled H(5). For this proton, an isotropic hyperfine-coupling constant of (−23 ± 1) MHz has been determined by continuous-wave EPR[21] and pulsed Davies ENDOR spectroscopy.

Virtually no variation of the line width is observed at the outer features of the spectrum upon deuteration of the buffer. Hence, hyperfine couplings due to nitrogens and nonexchangeable protons in FADH• mostly account for the line width in these spectral regions. Moreover, no line broadening is observed when the EPR detection frequency is increased from 94.5 GHz[21] to 360.03 GHz. Therefore, large **g**-strain effects which would give rise to a frequency-proportional broadening of the overall signal can be safely excluded up to frequencies of 360 GHz. This indicates that the FADH• radical in DNA photolyase has a well-defined environment and structural heterogeneities of the protein, which would give rise to **g**- or **A**-strain, are not prominent.

Apart from the magnitude of the **g**-tensor principal values, the orientation of the respective **g**-tensor principal axes provides important information which is required to understand, e.g., the various spin-polarized radical pair EPR signals with transient flavin radicals involved, observed in photolyases[45−50] or, e.g., to deduce the radical orientations from single-crystal studies. The orientation of the in-plane **g**-tensor axes *X* and *Y* can be obtained relative to the hyperfine tensor axes of the H(5) α-proton directly attached to the π-system, which is known to

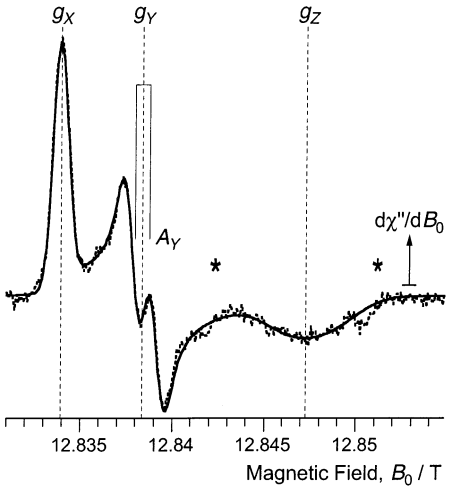

Figure 3. Comparison of calculated (drawn line) and experimental (dots) 360.03-GHz EPR spectra of the neutral flavin radical cofacor of DNA photolyase from *E. coli*. The calculated trace is the best fit using the **g**- and hyperfine values given in Table 1. The splitting at the g_Y feature is due to the projection of the H(5) hyperfine coupling component A_y onto the *Y* principal axis of **g**. The regions marked with asterisks contain small artifacts due to the field standard lines and were suppressed in the fitting routine with a zero-weight factor.

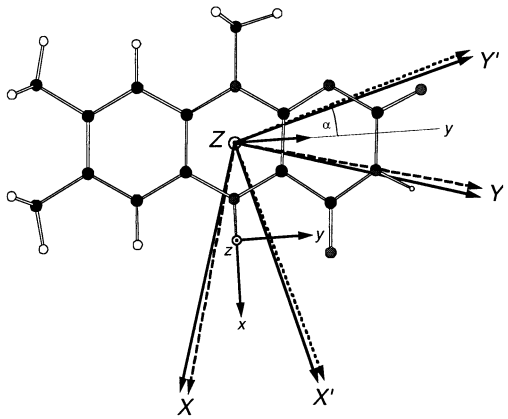

Figure 4. Molecular structure of the neutral flavin radical and **g**-tensor axes orientations. *X*, *Y*, and *Z* are the principal axes of the **g**-tensor (arrows with drawn lines: from experiment; arrows with dashed lines: from DFT calculation; arrows with dotted lines: from semiempirical AM1 calculation). *x*, *y*, and *z* are the directions of the molecular frame which coincides with the H(5) hyperfine tensor principal axes system. α is the angle between *X* and *x* or *Y* and *y* (for details, see text).

exhibit a large anisotropy within the molecular plane.[44] For an isolated C−H or N−H fragment, where C or N is a carbon or nitrogen of the π-system, respectively, the largest (negative) proton hyperfine tensor component is expected to be in the molecular plane, perpendicular to the C−H or N−H bond (the C−H or N−H bond is usually designated the *x*-direction, and *z* is the direction perpendicular to the molecular plane; *z* || *Z*, see Figure 4) (ref 71, pp 103). Principal values of $\mathbf{A}_{H(5)}$ have been obtained from pulsed 9-GHz Davies ENDOR experiments on the flavin cofactor in DNA photolyase in frozen solution: $A_x = -0.304$ mT, $A_z = -0.893$ mT, and $A_y = -1.33$ mT. Since the observed hyperfine splitting of (−)1.30 mT at the g_Y-edge is almost as large as the largest principal value of $\mathbf{A}_{H(5)}$, the **g**-axis corresponding to the principal value g_Y must be oriented roughly parallel to the molecular *y*-axis. The small deviation of the splitting at g_Y from the A_y-value determined by ENDOR must then be due to a tilt α of the (molecule-fixed) hyperfine tensor principal axes with respect to those of the **g**-tensor (see below).

TABLE 2: Comparison of Experimental and Calculated g-Tensor Principal Values for the Neutral Flavin Radical

	g_X	g_Y	g_Z
experimental values	2.004 31(5)	2.003 60(5)	2.002 17(7)
DFT calculation	2.004 98	2.004 46	2.002 07
AM1 calculation	2.004 00	2.003 43	2.002 16

Fitting of the 360.03-GHz EPR spectrum (Figure 2, trace A) was performed using two anisotropic ^{14}N hyperfine tensors taken from DFT studies[44] ($\mathbf{A}_{N(5)}$ and $\mathbf{A}_{N(10)}$, see Table 1) and the H(5) hyperfine tensor obtained from pulsed 9-GHz Davies ENDOR as fixed parameters. The nitrogens N(5) and N(10) are the major contributors to the significant inhomogeneous broadening of the g_Z-edge of the EPR spectrum. Any further unresolved couplings were taken into account through a (variable) orientation-dependent line width Γ_i, $i \in \{X, Y, Z\}$ where to a first approximation the line width variation was assumed to be collinear with the **g**-tensor. The best fit (Figure 3) of the spectrum yielded, in addition to the **g**-tensor principal values and the line widths Γ_i, the tilt angle $|\alpha| = (16 \pm 2)°$ between the Y and y axes, see Figure 4. To determine the sign of α, however, further information is required. This may be obtained by performing either (experimentally not yet feasible) high-frequency EPR studies on oriented samples or by comparing the experimentally obtained principal axes with those from quantum-chemical calculations of the **g**-tensor. We have followed the latter course, the results of which are described below.

The DFT and AM1-calculated principal values of **g** are given in Table 2 together with the experimental results. In accord with Stone's theory,[62] the orientation of the principal axis corresponding to the smallest **g**-tensor component, g_Z, of both computations, DFT and AM1, is perpendicular to the molecular plane, i.e., $Z \,||\, z$. Then again, two different orientations within the π-plane were obtained for the **g**-tensor X axis (and correspondingly also the Y axis): $\alpha = +17°$ is predicted from the semiempirical AM1 computation, whereas $\alpha = -14°$ is obtained from DFT (Figure 4). We prefer the latter value as it can be rationalized within the frame of **g**-tensor theory, where the largest principal value, g_X, is expected to be observed in a direction bisecting the smaller angle between the two axes along the C(2)═O(2) and C(4)═O(4) double bonds. The contribution of lone-pair electron excitations from the oxygens to Δg_X (and Δg_Y) is expected to dominate that from N(1) because of the smaller ξ of nitrogen and the low π-spin density at the N(1)-position. Moreover, the effect of O(4) should be stronger than that of O(2) due to the higher π-spin density at O(4) compared to that at O(2),[44] and hence, X is expected to lie closer to the C(4)═O(4) axis, as is obtained experimentally ($\alpha = ((-)16 \pm 2)°$). Certainly, experimental confirmation of this assignment has to await orientation-dependent submillimeter EPR experiments on single crystals, which, however, are not yet feasible.

A comparison of experimental and calculated **g** principal values, Table 2, reveals that DFT at the ZORA level of theory clearly overestimates the deviations of the g_i, $i \in \{X, Y, Z\}$ components from the free-electron value. In a recent study, scaling of Δg_i yielded good correlation between experimental and theoretical **g**-tensors for a set of small radicals.[72] Applying the suggested scaling factor (1/1.533) results in **g** principal values ($g_X = 2.004\,05$, $g_Y = 2.003\,72$, $g_Z = 2.002\,16$) that are slightly closer to the experimental data than those calculated by the AM1 method. Nonetheless, the Δg_X and Δg_Y anisotropies obtained from both quantum-chemical **g**-tensor calculations, DFT (after scaling) and AM1, are smaller than observed experimentally. Whether this is due to the neglect of environmental effects such as hydrogen bonding to FADH$^\bullet$ or due to systematic inaccuracies in the invoked calculations is a question that will be addressed in a future study.

Conclusions

Accurate **g**-tensor principal values were determined, for the first time, for a protein-associated neutral flavin radical. The relative orientation of the principal axes with respect to the molecular frame could be determined from the experiment with a small remaining ambiguity in the sign of the tilt angle ($\pm$ 16°) of the **g**-tensor around the molecular z-axis. MO calculations of **g** were not conclusive to definitely resolve this ambiguity. The likely tilt direction was rationalized taking into account the main contributions of the C═O bonds. The data obtained are important for EPR identification and understanding of catalytically active flavin radicals in photolyases and other flavoenzymes. Furthermore, knowledge of the principal axes of **g** with respect to the molecular structure of neutral flavin semiquinones paves the way for quantitative simulations of radical pair EPR spectra with flavin radical partners for a variety of redox-active flavoenzymes.

The **g**-tensor components contain subtle information on the electronic structure of the flavin radical, which can only be revealed if the anisotropy of **g** is resolved. Because the **g**-anisotropy of the FADH$^\bullet$ radical in DNA photolyase is extremely small, it was essential for this task to apply high-field EPR at microwave frequencies as high as 360 GHz. The Zeeman magnetoselection at such high magnetic fields is sufficient to isolate orientation-dependent subensembles of the nonoriented frozen sample. Hence, it should be feasible to obtain single-crystal like hyperfine information by ENDOR at 360 GHz/14 T even for disordered radicals with extremely small **g**-anisotropy. Work along these lines is in progress at the Free University Berlin.

Acknowledgment. This work was supported by the Deutsche Forschungsgemeinschaft (SFB-498 [for EPR/ENDOR studies and DFT calculations], SPP-1055 "High-Field EPR in Biology, Chemistry, and Physics" [for high-field EPR instrumentation], and SFB-533 [for molecular biology and protein chemistry]) and the Fonds der Chemischen Industrie, which is gratefully acknowledged.

References and Notes

(1) Bruice, T. C. *Acc. Chem. Res.* **1980**, *13*, 256.
(2) Müller, F. *Top. Curr. Chem.* **1983**, *108*, 71.
(3) Ghisla, S.; Massey, V. *Eur. J. Biochem.* **1989**, *181*, 1.
(4) Fraaije, M. W.; Mattevi, A. *Trends Biochem. Sci.* **2000**, *25*, 126.
(5) Edmondson, D. E.; Tollin, G. *Top. Curr. Chem.* **1983**, *108*, 109.
(6) Sancar, G. B. *Mutat. Res.* **1990**, *236*, 147.
(7) Sancar, G. B. *Mutat. Res.* **2000**, *451*, 25.
(8) Sancar, A. *Biochemistry* **1994**, *33*, 2.
(9) Zhao, X.; Mu, D. *Histol. Histopathol.* **1998**, *13*, 1179.
(10) Todo, T. *Mutat. Res.* **1999**, *434*, 89.
(11) Deisenhofer, J. *Mutat. Res.* **2000**, *460*, 143.
(12) Carell, T.; Burgdorf, L. T.; Kundu, L. M.; Cichon, M. *Curr. Opinion Chem. Biol.* **2001**, *5*, 491.
(13) Eriksson, L. E. G.; Ehrenberg, A. *Acta Chem. Scand.* **1964**, *18*, 1437.
(14) Ehrenberg, A.; Eriksson, L. E. G.; Hyde, J. S. *Biochim. Biophys. Acta* **1968**, *167*, 482.
(15) Kurreck, H.; Bock, M.; Bretz, N.; Elsner, M.; Kraus, H.; Lubitz, W.; Müller, F.; Geissler, J.; Kroneck, P. M. H. *J. Am. Chem. Soc.* **1984**, *106*, 737.
(16) Kurreck, H.; Bretz, N. H.; Helle, N.; Henzel, N.; Weilbacher, E. *J. Chem. Soc., Faraday Trans. 1* **1988**, *84*, 3293.
(17) Medina, M.; Vrielink, A.; Cammack, R. *Eur. J. Biochem.* **1994**, *222*, 941.
(18) Medina, M.; Gómez-Moreno, C.; Cammack, R. *Eur. J. Biochem.* **1995**, *227*, 529.

(19) DeRose, V. J.; Woo, J. C. G.; Hawe, W. P.; Hoffman, B. M.; Silverman, R. B.; Yelekci, K. *Biochemistry* **1996**, *36*, 11 085.
(20) Çinkaya, I.; Buckel, W.; Medina, M.; Gómez-Moreno, C.; Cammack, R. *Biol. Chem.* **1997**, *378*, 843.
(21) Kay, C. W. M.; Feicht, R.; Schulz, K.; Sadewater, P.; Sancar, A.; Bacher, A.; Möbius, K.; Richter, G.; Weber, S. *Biochemistry* **1999**, *38*, 16740.
(22) Weber, S.; Richter, G.; Schleicher, E.; Bacher, A.; Möbius, K.; Kay, C. W. M. *Biophys. J.* **2001**, *81*, 1195.
(23) Martínez, J. I.; Alonso, P. J.; Gómez-Moreno, C.; Medina, M. *Biochemistry* **1997**, *36*, 15 526.
(24) Medina, M.; Vrielink, A.; Cammack, R. *FEBS Lett.* **1997**, *400*, 247.
(25) Medina, M.; Lostao, A.; Sancho, J.; Gómez-Moreno, C.; Cammack, R.; Alonso, P. J.; Martínez, J. I. *Biophys. J.* **1999**, *77*, 1712.
(26) Stevenson, R. C.; Dunham, W. R.; Sands, R. H.; Singer, T. P.; Beinert, H. *Biochim. Biophys. Acta* **1986**, *869*, 81.
(27) Fournel, A.; Gambarelli, S.; Guigliarelli, B.; More, C.; Asso, M.; Chouteau, G.; Hille, R.; Bertrand, P. *J. Chem. Phys.* **1998**, *109*, 10 905.
(28) Grinberg, O. Y.; Dubinskii, A. A.; Lebedev, Y. S. *Russ. Chem. Rev. (Engl. Transl.)* **1983**, *52*, 850.
(29) Lynch, W. B.; Earle, K. A.; Freed, J. H. *Rev. Sci. Instrum.* **1988**, *59*, 1345.
(30) Weber, R. T.; Disselhorst, J. A.; Prevo, L. J.; Schmidt, J.; Wenckebach, W. T. *J. Magn. Reson.* **1989**, *81*, 129.
(31) Prisner, T. F.; Un, S.; Griffin, R. G. *Israel J. Chem.* **1992**, *32*, 357.
(32) Burghaus, O.; Rohrer, M.; Götzinger, T.; Plato, M.; Möbius, K. *Meas. Sci. Technol.* **1992**, *3*, 765.
(33) Müller, F.; Hopkins, M. A.; Coron, N.; Grynberg, M.; Brunel, L.-C.; Martinez, G. *Rev. Sci. Instrum.* **1989**, *60*, 3681.
(34) Earle, K. A.; Tipikin, D. S.; Freed, J. H. *Rev. Sci. Instrum.* **1996**, *67*, 2502.
(35) Reijerse, E. J.; Dam, P. J. v.; Klaassen, A. A. K.; Hagen, W. R.; Bentum, P. J. M. v.; Smith, G. M. *Appl. Magn. Reson.* **1998**, *14*, 153.
(36) Smith, G. M.; Lesurf, J. C. G.; Mitchell, R. H.; Riedi, P. C. *Rev. Sci. Instrum.* **1998**, *69*, 3924.
(37) Moll, H. P.; Kutter, C.; Tol, J. v.; Zuckerman, H.; Wyder, P. *J. Magn. Reson.* **1999**, *137*, 46.
(38) Rohrer, M.; Krzystek, J.; Williams, V.; Brunel, L.-C. *Meas. Sci. Technol.* **1999**, *10*, 275.
(39) Cardin, J. T.; Kolaczkowski, S. V.; Anderson, J. R.; Budil, D. E. *Appl. Magn. Reson.* **1999**, *16*, 273.
(40) Fuchs, M.; Prisner, T. F.; Möbius, K. *Rev. Sci. Instrum.* **1999**, *70*, 3681.
(41) Jorns, M. S.; Sancar, G. B.; Sancar, A. *Biochemistry* **1984**, *23*, 2673.
(42) Jorns, M. S.; Wang, B.; Jordan, S. P.; Chanderkar, L. P. *Biochemistry* **1990**, *29*, 552.
(43) Payne, G.; Heelis, P. F.; Rohrs, B. R.; Sancar, A. *Biochemistry* **1987**, *26*, 7121.
(44) Weber, S.; Möbius, K.; Richter, G.; Kay, C. W. M. *J. Am. Chem. Soc.* **2001**, *123*, 3790.
(45) Kim, S.-T.; Sancar, A.; Essenmacher, C.; Babcock, G. T. *J. Am. Chem. Soc.* **1992**, *114*, 4442.
(46) Kim, S.-T.; Sancar, A.; Essenmacher, C.; Babcock, G. T. *Proc. Natl. Acad. Sci. U.S.A.* **1993**, *90*, 8023.
(47) Essenmacher, C.; Kim, S.-T.; Atamian, M.; Babcock, G. T.; Sancar, A. *J. Am. Chem. Soc.* **1993**, *115*, 1602.
(48) Rustandi, R. R.; Jorns, M. S. *Biochemistry* **1995**, *34*, 2284.
(49) Gindt, Y. M.; Vollenbroek, E.; Westphal, K.; Sackett, H.; Sancar, A.; Babcock, G. T. *Biochemistry* **1999**, *38*, 3857.
(50) Weber, S.; Kay, C. W. M.; Mögling, H.; Möbius, K.; Hitomi, K.; Todo, T. *Proc. Natl. Acad. Sci. U.S.A.* **2002**, *99*, 1319.
(51) Wang, B.; Jorns, M. S. *Biochemistry* **1989**, *28*, 1148.
(52) Earle, K. A.; Budil, D. E.; Freed, J. H. *J. Phys. Chem.* **1993**, *97*, 13 289.
(53) Nilges, M. J. Electron Paramagnetic Resonance Studies of Low Symmetry Nickel(I) and Molybdenum(V) Complexes, Ph.D. Thesis, University of Illinois, 1979.
(54) Veen, G. V. *J. Magn. Reson.* **1978**, *30*, 91.
(55) Morin, G.; Bonnin, D. *J. Magn. Reson.* **1999**, *136*, 176.
(56) Barone, V. Recent Advances in Density-Functional Methods, Part I.; Chong, D. P., Ed.; World Scientific Publishing: Singapore, 1995.
(57) Rega, N.; Cossi, M.; Barone, V. *J. Chem. Phys.* **1996**, *105*, 11 060.
(58) Becke, A. D. *J. Chem. Phys.* **1993**, *98*, 5648.
(59) Frisch, M. J.; Trucks, G. W.; Schlegel, H. B.; Scuseria, G. E.; Robb, M. A.; Cheeseman, J. R.; Zakrzewski, V. G.; Montgomery, J. A.; Stratmann, R. E.; Burant, J. C.; Dapprich, S.; Millam, J. M.; Daniels, A. D.; Kudin, K. N.; Strain, M. C.; Farkas, O.; Tomasi, J.; Barone, V.; Cossi, M.; Cammi, R.; Mennucci, B.; Pomelli, C.; Adamo, C.; Clifford, S.; Ochterski, J.; Petersson, G. A.; Ayala, P. Y.; Cui, Q.; Morokuma, K.; Malick, D. K.; Rabuck, A. D.; Raghavachari, K.; Foresman, J. B.; Cioslowski, J.; Ortiz, J. V.; Stefanov, B. B.; Liu, G.; Liashenko, A.; Piskorz, P.; Komaromi, I.; Gomperts, R.; Martin, R. L.; Fox, D. J.; Keith, T.; Al-Laham, M. A.; Peng, C. Y.; Nanayakkara, C.; Gonzalez, M.; Challacombe, M.; Gill, P. M. W.; Johnson, B. G.; Chen, W.; Wong, M. W.; Andres, J. L.; Head-Gordon, M.; Replogle, E. S.; Pople, J. A. *Gaussian 98*; revision A.7, 1998.
(60) Törring, J. T.; Un, S.; Knüpling, M.; Plato, M.; Möbius, K. *J. Chem. Phys.* **1997**, *107*, 3905.
(61) Dewar, M. J. S.; Zoebisch, E. G.; Healy, E. F.; Stewart, J. J. P. *J. Am. Chem. Soc.* **1985**, *107*, 3902.
(62) Stone, A. J. *Proc. R. Soc. London* **1963**, *A 271*, 424.
(63) Baerends, E. J.; Ellis, D. E.; Ros, P. *Chem. Phys.* **1973**, *2*, 41.
(64) Versluis, L.; Ziegler, T. *J. Chem. Phys.* **1988**, *88*, 322.
(65) Velde, G. t.; Baerends, E. J. *J. Comput. Phys.* **1992**, *99*, 84.
(66) Guerra, C. F.; Snijders, J. G.; Velde, G. t.; Baerends, E. J. *Theor. Chem. Acc.* **1998**, *99*, 391.
(67) Lenthe, E. v.; Snijders, J. G.; Baerends, E. J. *J. Chem. Phys.* **1996**, *105*, 6505.
(68) Lenthe, E. v.; Wormer, P. E. S.; Avoird, A. v. d. *J. Chem. Phys.* **1997**, *107*, 2488.
(69) Becke, A. D. *Phys. Rev. A* **1988**, *38*, 3098.
(70) Perdew, J. P. *Phys. Rev. B* **1986**, *33*, 8822.
(71) Carrington, A.; McLachlan, A. D. *Introduction to Magnetic Resonance*; Harper & Row: New York, 1967.
(72) Neese, F. *J. Chem. Phys.* **2001**, *115*, 11 080.